POLITECNICO DI TORINO
Repository ISTITUZIONALE

Low-Complexity Sequential LMBA for FR1 5G NR

Original
Low-Complexity Sequential LMBA for FR1 5G NR / Shi, P., Zuloaga, L.C., Bartolotti, G., Zhang, Z., Piacibello, A., Garcia, J.A., Camarchia, V.. - ELETTRONICO. - (2025), pp. 19-22. (2025 IEEE Topical Conference on RF/Microwave Power Amplifiers for Radio and Wireless Applications, PAWR 2025 San Juan (USA) 19-22 January 2025) [10.1109/pawr63954.2025.10904059].

Availability:
This version is available at: 11583/3017250 since: 2026-10-30T16:46:54Z

Publisher:
Institute of Electrical and Electronics Engineers Inc.

Published
DOI:10.1109/pawr63954.2025.10904059

Terms of use:

This article is made available under terms and conditions as specified in the corresponding bibliographic description in the repository

Publisher copyright
IEEE postprint/Author's Accepted Manuscript

©2025 IEEE. Personal use of this material is permitted. Permission from IEEE must be obtained for all other uses, in any current or future media, including reprinting/republishing this material for advertising or promotional purposes, creating new collecting works, for resale or lists, or reuse of any copyrighted component of this work in other works.

(Article begins on next page)

10 November 2026

Low-Complexity Sequential LMBA for FR1 5G NR

Peiyuan Shi
Politecnico di Torino
Torino, Italy
peiyuan.shi@studenti.polito.it

Luis Crespo Zuloaga
Universidad de Cantabria
Santander, España
luis.crespoz@alumnos.unican.es

Giulia Bartolotti
Politecnico di Torino
Torino, Italy
giulia.bartolotti@polito.it

Zhifan Zhang
Politecnico di Torino
Torino, Italy
zhifan.zhang@polito.it

Anna Piacibello
Politecnico di Torino
Torino, Italy
anna.piacibello@polito.it

Jose Angel Garcia
Universidad de Cantabria
Santander, España
joseangel.garcia@unican.es

Vittorio Camarchia
Politecnico di Torino
Torino, Italy
vittorio.camarchia@polito.it

***Abstract*—This paper presents the design and characterization of an SLMBA targeting 10-dB back-off efficiency enhancement in the N78 (3.3–3.8 GHz) 5G band. The design aims at minimizing complexity by adopting identical transistors in all branches and the same drain supply voltage. The prototype delivers more than 44 dBm saturated output power while maintaining efficiency higher than 56% and 34% at saturation and 10 dB back-off, respectively. This confirms the validity of the approach in providing performance in line with the current state of the art.**

***Index Terms*—Broadband, Efficiency enhancement, LMBA, Power amplifier, 5G.**

I. Introduction

Conventional Power Amplifiers (PAs) typically achieve their highest efficiency at output saturation. However, with the increasing prevalence of high-Peak to Average Power Ratio (PAPR) signals, this approach is no longer suitable for modern communication systems. The challenge is to develop PAs that can boost efficiency before reaching output power saturation, addressing the need for high efficiency in the Output Back-Off (OBO) region. The Doherty PA is one of the most popular architectures in this context, both in the FR1 and FR2 bands, successfully achieving efficiency enhancement at 6 dB as well as deeper OBO [1]–[3]. This architecture lends itself to both single- and dual-input implementations [4], [5]. Recently, the Load Modulated Balanced Amplifier (LMBA) architecture has been introduced as dual-input architecture and then developed in various forms, both single- and dual-input [6]–[8]. One promising variant is the Sequential LMBA (SLMBA), which explores the possibility of extending efficiency into deeper OBO regions. A key feature of the SLMBA is that no load modulation happens at the Carrier Amplifier (CA), which is beneficial for wideband operation. At the same time it is prone to deep-OBO operation because the class-C balanced stage has typically a larger periphery than the class-AB CA.

This paper presents an SLMBA able to cover the full N78 5G NR bandwidth (3.3–3.8 GHz). The prototype is able to maintain a saturated power in excess of 44 dBm with efficiency higher than 56 % and 34 % at saturation and 10 dB OBO, respectively, placing it well in line with the present state of the art.

II. Design Strategy

The SLMBA (see block diagram of Fig. 1) is composed of a Balanced Amplifier (BA) with two identical devices biased in Class-C, and a carrier amplifier (CA) biased in Class-AB injecting power in the isolated port of the output quadrature coupler. The single RF input is split among the two branches, and the proper phase alignment, required to get constructive signal interference at the output, is ensured by a phase compensator. At low power, the BA remains off, and only the CA contributes to the output power. The BA is designed to turn on as the CA approaches saturation, which provides additional power to the output load and enhances efficiency, thereby improving the overall performance of the amplifier, especially in handling high-PAPR signals.

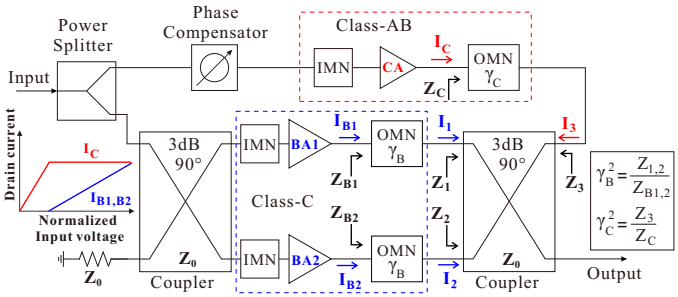


Fig. 1. Block diagram of the SLMBA.

This design targets a saturated power of 44 dBm with 9/10-dB OBO efficiency enhancement in the 3.3–3.8 GHz band. Based on the theory outlined in [9], [10], design equations of the combiner parameters are derived as functions of the specified design parameters ($P_{\mathrm{OUT,sat}}$, OBO).

The individual power contributions of the two branches are:

$$P_{\mathrm{C,sat}} = \frac{P_{\mathrm{OUT,sat}}}{\mathrm{OBO}}, \qquad P_{\mathrm{B,sat}} = (\mathrm{OBO} - 1) \cdot P_{\mathrm{C,sat}}, \quad (1)$$

where $P_{\mathrm{C,sat}}$ is the saturated power of the CA and $P_{\mathrm{B,sat}} = 2 \cdot P_{\mathrm{B1,sat}}$ is the total power of the BA.

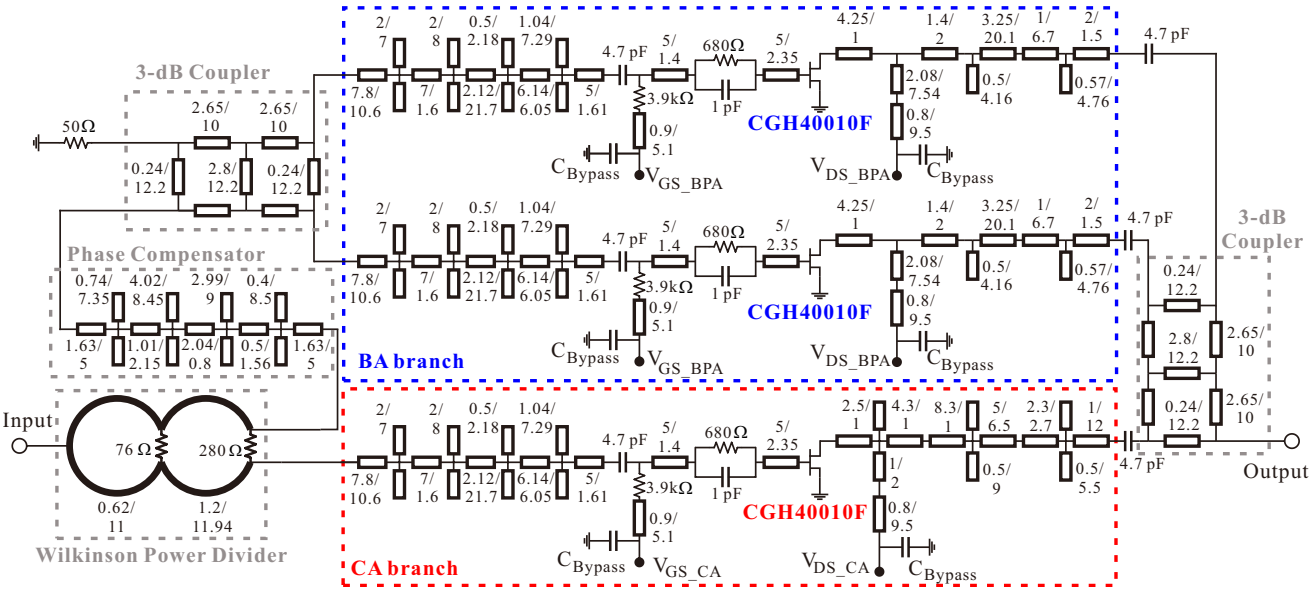


Fig. 2. Overall schematic of the presented SLMBA. Lines dimensions are specified as Width/Length in mm

The drain currents at the current generator (CG) planes and the corresponding optimum impedances are then derived as:

$$I_{\mathrm{C,B}_{1,2}} = \frac{2 \cdot P_{\mathrm{C,B}_{1,2},\mathrm{sat}}}{V_{\mathrm{C,B}_{1,2}}}, \qquad R_{\mathrm{opt,C,B}_{1,2}} = \frac{V_{\mathrm{C,B}_{1,2}}}{I_{\mathrm{C,B}_{1,2}}}, \tag{2}$$

where $V_{\mathrm{C,B}_{1,2}}$ denotes the drain voltages at the same planes of CA and BA, respectively.

Since the impedance at port 3 of the coupler is not modulated and is equal to Z_0 throughout the whole dynamic range, the OMN of the CA has to transform it into the optimum impedance of the transistor according to the impedance transformation ratio:

$$\gamma_{\mathrm{C}} = \sqrt{\frac{Z_0}{R_{\mathrm{opt,C}}}}. \tag{3}$$

The impedances at the coupler ports 1,2, and correspondingly the one at the CG planes, instead, are modulated by the CA as:

$$Z_{1,2} = Z_0 \left(1 + \sqrt{2}\frac{I_3}{I_{1,2}}\right) \tag{4}$$

$$Z_{\mathrm{B}_{1,2}} = \frac{Z_0}{\gamma_{\mathrm{B}}^2}\left(1 + \sqrt{2}\frac{I_C \cdot \gamma_{\mathrm{B}}}{I_{\mathrm{B}_{1,2}} \cdot \gamma_{\mathrm{C}}}\right), \tag{5}$$

$$\text{where} \quad \gamma_{\mathrm{B}} = \sqrt{\frac{Z_{1,2}}{Z_{\mathrm{B}_{1,2}}}}. \tag{6}$$

The value of γ_{B} is computed from (1)–(6) as:

$$\gamma_{\mathrm{B}} = \frac{I_{\mathrm{B}1,2}}{I_{\mathrm{C}}} \cdot \frac{2\gamma_{\mathrm{C}}}{\sqrt{2 \cdot \mathrm{OBO}} - \sqrt{2}}. \tag{7}$$

For a 9/10-dB OBO SLMBA, $P_{\mathrm{C,sat}}$ results about 4 times smaller than $P_{\mathrm{B}_{1,2},\mathrm{sat}}$, which would call for different device sizes for an optimal power utilization. However, in this implementation, three identical 10 W packaged GaN devices (CGH40010F from Wolfspeed) with the same drain supply voltage are adopted. While this choice partially under-utilizes the CA, it reduces the complexity and simplifies the implementation. Using a unique device size and similar stabilization and matching networks is advantageous in terms of phase variation versus frequency, crucial for wideband operation. Having a single drain supply voltage minimizes complexity of the DC circuitry in the system, although this implies trading off OBO efficiency [11]. Additionally, since the CA is typically strongly compressed in SLMBAs, which may represent an issue for reliability, adopting a larger device may allow for a mild load modulation hence reducing the stress.

The coupler impedance Z_0 is a free parameter, which can lead to different design choices. If Z_0 is chosen to be 50 Ω, additional post-matching at the output can be avoided. However, this in general calls for output matching of both CA and BA. If the device output parasitics were negligible, Z_0 could be chosen in such a way to avoid inserting an OMN at the output of either CA ($\gamma_{\mathrm{C}} = 1$) or BA ($\gamma_{\mathrm{B}} = 1$), thus enhancing bandwidth and reducing circuit complexity. However, the adoption of packaged devices at frequencies where their parasitic effects have a strong impact makes OMNs unavoidable. Therefore, the optimal choice for minimum complexity is $Z_0 = 50\,\Omega$. Accounting for some output losses, especially due to mismatch and sub-optimal phase alignment, the circuit parameters are derived for a slightly over-estimated target of $P_{\mathrm{OUT,sat}} = 45$ dBm and OBO = 10 dB, and result into: $P_{\mathrm{C,sat}} = 3.2$ W, $I_{\mathrm{C}} = 0.23$ A, $R_{\mathrm{opt,C}} \approx 124\,\Omega$, $\gamma_{\mathrm{C}} = 0.64$ for the CA, and $P_{\mathrm{B}_{1,2},\mathrm{sat}} = 28.5$ W, $I_{\mathrm{B}_{1,2}} = 1.01$ A, $R_{\mathrm{opt,B}_{1,2}} \approx 27.5\,\Omega$, $\gamma_{\mathrm{B}} = 1.9$ for the BA. Consequently, wideband OMNs were designed to match the coupler plane impedances to the intrinsic CG plane's optimum loads. A 2-section LC model of the output parasitics of the transistors

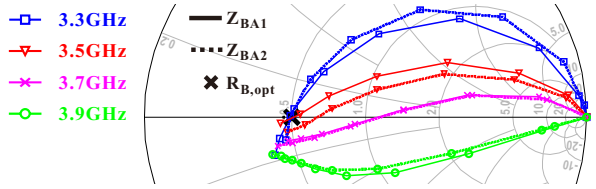


Fig. 3. Simulated load modulation trajectories of the BA at the current generator planes.

($C_1 = 0.68\,\text{pF}$, $L_1 = 0.34\,\text{nH}$, $C_2 = 0.94\,\text{pF}$, $L_2 = 0.54\,\text{nH}$) was extracted using the method reported in [12] and considered to be part of the OMNs. As previously determined, the difference between impedance transformation ratios γ_B and γ_C results in different orders and phase responses for the BA's and CA's OMNs across frequencies. This significantly affects the phase relationship between the BA and CA branches over the entire band. Thus, a phase compensator is mandatory to maintain the correct load modulation and power combination at the output coupler. Finally, a 4^{th} order filter matched to $50\,\Omega$ was implemented on the BA's branch. The stabilization network was designed to ensure unconditional small signal stability across both the low-frequency band and the operational band. To guarantee wideband performance, 2-section Wilkinson splitters and 2-section branchline couplers, all matched to $50\,\Omega$, were optimized and implemented.

Fig. 2 shows the overall schematic of the presented SLMBA, fabricated in a 0.8 mm-thick Rogers 4350B substrate, highlighting the main building blocks. The load modulation of the SLMBA prototype was simulated using the intrinsic nodes provided by the nonlinear model, with the load modulation trajectories of BA intrinsic load demonstrated in Fig. 3.

III. Fabrication and Characterization

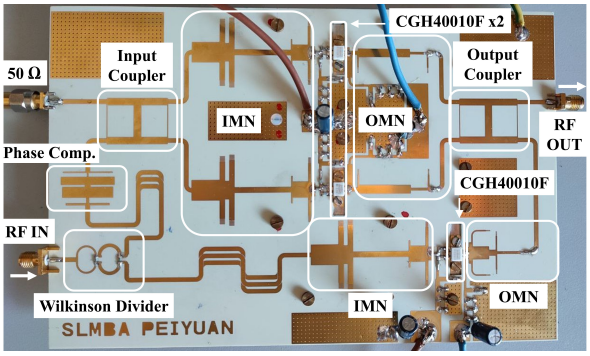


Fig. 4. Photograph of the SLMBA prototype.

The SLMBA demonstrator is shown in Fig. 4. It has been mounted on an aluminum carrier for heat dissipation. The characterization is performed at the following bias point: $V_{DD} = 28\,\text{V}$, $V_{GS,B} = -5\,\text{V}$, $V_{GS,C} = -2.55\,\text{V}$, for a 110 mA drain current.

Fig. 5 shows the small signal comparison of measurements and simulations. The input and output reflection coefficients

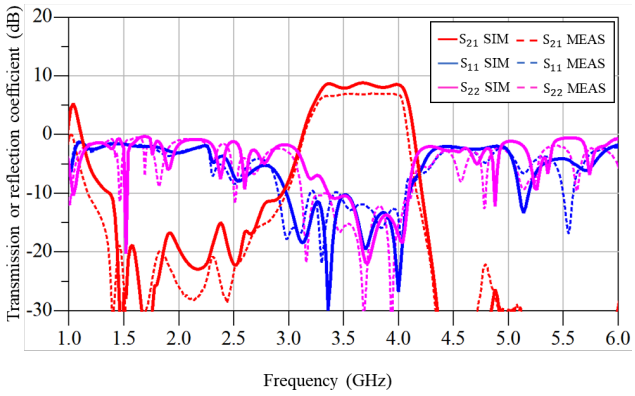


Fig. 5. Comparison between simulated and measured scattering parameters.

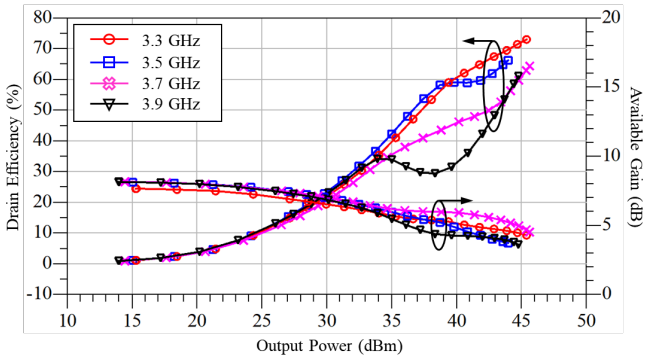


Fig. 6. Measured drain efficiency and gain versus output power.

are in good agreement with the simulations and are below -10 dB over the target frequency band. The measured S_{21} exhibits a flat behavior in band. However, the value is marginally lower (about 1 dB) than the simulated one, probably due to oxidization of the aluminum carrier causing a small parasitic source inductance.

The CW characterization has been performed from 3.2 GHz to 4 GHz with a real-time calibrated vector setup. Fig. 6 illustrates the efficiency and gain profiles versus output power at four frequency points, spaced by 200 MHz in the band. The efficiency is higher than 56% and 34% at saturation and at 10-dB OBO, respectively. The gain profiles show a good uniformity and achieve a compression of about 4 dB at saturation. Fig. 7 summarizes the measured performance versus frequency. The saturated power is higher than 44 dBm in the target bandwidth, which is compliant with the design specifications. The efficiency at saturation is higher than 56%, while it reaches 54/47/39% at 6-/8-dB/10-dB OBO, respectively.

The achieved performance is compared to the state of the art of LMBAs at similar frequencies in Table I. Most of the demonstrators target lower frequencies and are based on different device sizes [10], [13] or asymmetrical drain voltages [9], [11], which privileges the back-off efficiency but

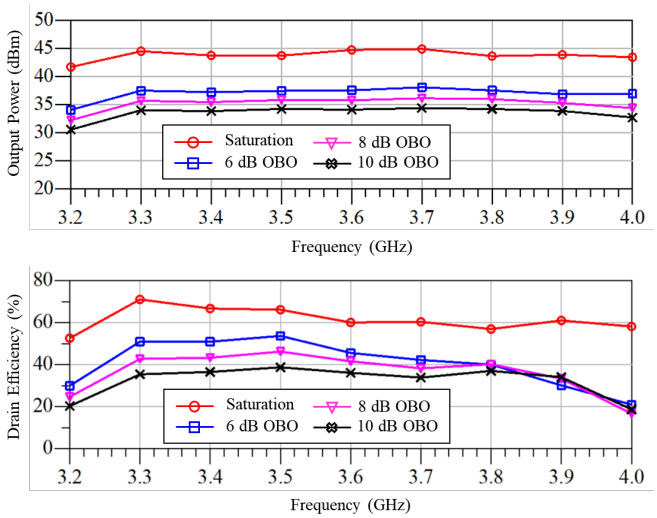


Fig. 7. Measured output power (top) and drain efficiency (bottom) versus frequency.

increases complexity. On the contrary, especially compared to [8] which operates in a similar band and uses different device sizes, the proposed strategy is beneficial for saturated efficiency and slightly sub-optimal for back-off efficiency. Finally, the gain performance is quite comparable among most of the works.

TABLE I
COMPARISON WITH THE STATE OF THE ART.

Ref.	Archit.	Freq. (GHz)	Gain (dB)	P_{sat} (dBm)	η_{sat} (%)	$\eta_{10\,\mathrm{dB}}$ (%)
[9]	SLMBA	3.05–3.55	9.5	43.7	61	43
[10]	PD-LMBA	1.5–2.7	6*	43	58	47
[8]	RF-in LMBA	3.1–4.2	7	48	47	47
[13]	APD-LMBA	2.5–2.9	5*	40	70	42
[11]	SLMBA	1.9–3.2	7.5*	43	47	42
T. W.	**SLMBA**	**3.3–3.9**	**7.5**	**44**	**56**	**34**

* Graphically estimated.

IV. CONCLUSION

A Sequential LMBA PA able to cover the full N78 5G NR band (3.3 GHz–3.8 GHz) has been presented. Adopting a unique device size and drain supply voltage for all the transistors, the prototype minimizes the complexity both at circuit and system level, while maintaining performance in line with the present state of the art.

ACKNOWLEDGEMENT

This research was partially supported by the Project Programma Operativo Nazionale (PON) Ricerca e Innovazione "Tecnologie abilitanti e architetture innovative per future generazioni (6G) di trasmettitori intelligenti green" (DM 1062/21, CUP E15F21003760001) funded by the Italian Ministry of University and Research (MUR).

REFERENCES

[1] H. Zhou, J.-R. Perez-Cisneros, S. Hesami, K. Buisman, and C. Fager, "A Generic Theory for Design of Efficient Three-Stage Doherty Power Amplifiers," *IEEE Trans. Microw. Theory Techn.*, vol. 70, no. 2, pp. 1242–1253, 2022.

[2] A. Piacibello, R. Quaglia, R. Giofrè, R. Figueiredo, P. Colantonio, N. B. Carvalho, V. Valenta, and V. Camarchia, "High-Gain and High-Linearity MMIC GaN Doherty Power Amplifier With 3-GHz Bandwidth for Ka-Band Satellite Communications," *IEEE Microwave and Wireless Technology Letters*, vol. 34, no. 6, pp. 765–768, 2024.

[3] R. Giofrè, A. Piacibello, V. Camarchia, and P. Colantonio, "A Two-Way GaN Doherty Amplifier for 5G FR2 With Extended Back-Off Range," *IEEE Microwave and Wireless Technology Letters*, vol. 34, no. 3, pp. 314–317, 2024.

[4] C. M. Andersson, D. Gustafsson, J. Chani Cahuana, R. Hellberg, and C. Fager, "A 1–3-GHz Digitally Controlled Dual-RF Input Power-Amplifier Design Based on a Doherty-Outphasing Continuum Analysis," *IEEE Trans. Microw. Theory Techn.*, vol. 61, no. 10, pp. 3743–3752, 2013.

[5] A. Piacibello, R. Quaglia, V. Camarchia, C. Ramella, and M. Pirola, "Dual-input driving strategies for performance enhancement of a Doherty power amplifier," in *2018 IEEE MTT-S International Wireless Symposium (IWS)*, 2018, pp. 1–4.

[6] D. J. Shepphard, J. Powell, and S. C. Cripps, "An efficient broadband reconfigurable power amplifier using active load modulation," *IEEE Microwave and Wireless Components Letters*, vol. 26, no. 6, pp. 443–445, 2016.

[7] R. Quaglia, J. Pang, S. C. Cripps, and A. Zhu, "Load-modulated balanced amplifier: From first invention to recent development," *IEEE Microwave Magazine*, vol. 23, no. 12, pp. 60–70, 2022.

[8] P. Saad and R. Hou, "Symmetrical load modulated balanced power amplifier with asymmetrical output coupling for load modulation continuum," *IEEE Trans. Microw. Theory Techn.*, vol. 70, no. 4, pp. 2315–2327, 2022.

[9] J. Pang, Y. Li, M. Li, Y. Zhang, X. Y. Zhou, Z. Dai, and A. Zhu, "Analysis and design of highly efficient wideband rf-input sequential load modulated balanced power amplifier," *IEEE Trans. Microw. Theory Techn.*, vol. 68, no. 5, pp. 1741–1753, 2020.

[10] Y. Cao and K. Chen, "Pseudo-doherty load-modulated balanced amplifier with wide bandwidth and extended power back-off range," *IEEE Trans. Microw. Theory Techn.*, vol. 68, no. 7, pp. 3172–3183, 2020.

[11] P. Chen, L. Qi, J. Xia, R.-J. Liu, J. Chen, L. Yu, X.-W. Zhu, C. Yu, and W. Hong, "A theoretical method to optimize the control signal power for high-efficiency symmetrical load modulated balanced amplifier designs," *IEEE Microwave and Wireless Technology Letters*, vol. 34, no. 2, pp. 211–214, 2024.

[12] M. Li, J. Pang, Y. Li, and A. Zhu, "Ultra-wideband dual-mode doherty power amplifier using reciprocal gate bias for 5g applications," *IEEE Trans. Microw. Theory Techn.*, vol. 67, no. 10, pp. 4246–4259, 2019.

[13] J. Chen, L. Yu, R.-J. Liu, P. Chen, and C. Yu, "Design of an asymmetrical pseudo-doherty load-modulated balanced amplifier with 15-db back-off high efficiency," in *2023 IEEE International Conference on Integrated Circuits, Technologies and Applications (ICTA)*, 2023, pp. 136–137.